Earth and Planetary Science Letters 383 (2013) 101–112

Contents lists available at ScienceDirect

Earth and Planetary Science Letters

www.elsevier.com/locate/epsl

Millennial-scale Agulhas Current variability and its implications for salt-leakage through the Indian–Atlantic Ocean Gateway

Margit H. Simon [a,*], Kristina L. Arthur [b], Ian R. Hall [a], Frank J.C. Peeters [b], Benjamin R. Loveday [c], Stephen Barker [a], Martin Ziegler [a,d], Rainer Zahn [e,f]

[a] School of Earth and Ocean Sciences, Cardiff University, Cardiff, CF10 3AT, United Kingdom
[b] Vrije Universiteit Amsterdam, Faculty of Earth- and Life Sciences, De Boelelaan 1105, 1081 HV Amsterdam, The Netherlands
[c] Department of Oceanography, University of Cape Town, Rondebosch, Cape Town, South Africa
[d] Department of Earth Sciences, Eidgenössische Technische Hochschule Zürich, CH-8092 Zürich, Switzerland
[e] Institució Catalana de Recerca i Estudis Avançats (ICREA), 08010 Barcelona, Spain
[f] Institut de Ciència i Tecnologia Ambientals (ICTA), y Departament de Física, Universitat Autònoma de Barcelona, 08193 Bellaterra, Spain

ARTICLE INFO

Article history:
Received 21 June 2013
Received in revised form 20 September 2013
Accepted 22 September 2013
Available online 17 October 2013
Editor: J. Lynch-Stieglitz

Keywords:
Agulhas Current
Agulhas leakage
millennial-scale
southwest Indian Ocean sub-gyre
Southern Hemisphere westerlies

ABSTRACT

The inter-ocean exchange of warm and salt-enriched waters around South Africa (Agulhas leakage), may have played an important role in the mechanism of deglaciations. Paleoceanographic reconstructions from the Agulhas leakage corridor show that leakage maxima occurred during glacial terminations. Therefore enhanced leakage has been suggested as a forcing mechanism to shift the Atlantic Meridional Overturning Circulation into the interglacial mode of circulation. At present, studies have not considered that upstream changes in the properties of the Agulhas Current itself may, in part, explain the observed variability in the Agulhas leakage and play an important role in defining the upper ocean hydrography of the South Atlantic. Here, we present a multi-proxy record from a marine sediment core (CD154 17-17K) located in the main trajectory of the Agulhas Current that spans the past 100 kyr. The record shows considerable variability in reconstructed upper ocean temperatures and salinity. We also find that the relative abundance of tropical and sub-tropical planktic foraminifera, previously used as a proxy for Agulhas leakage fauna, shows considerable upstream variability, likely reflecting changes in the hydrography of the southwest Indian Ocean sub-gyre (SWIOSG) and upper ocean temperatures. Idealised numerical model simulations demonstrate that both a shifting and an intensification of the Southern Hemisphere westerlies modify the vigour of the SWIOSG. These changes also drive increased kinetic and eddy variability in the Agulhas Return Current that potentially enhances cross frontal mixing of southern sourced waters into the SWIOSG system. Our results suggest that variability in the upstream Agulhas Current hydrography is strongly linked to the dynamics of the Agulhas Return Current and strength of the SWIOSG and that downstream variability in the leakage area (Atlantic sector) at least partly reflects regional variations of the Agulhas Current as a whole.

1. Introduction

The world's largest western boundary current, the Agulhas Current, is part of the subtropical Indian Ocean gyre (STIOG) and transports about 70–78 Sv (1 Sv = 10^6 m^3 s^{-1}) of tropical and subtropical waters along the eastern margin of southern Africa (Lutjeharms, 2006). At the southern tip of Africa, between 15°E and 20°E, the current retroflects with the majority of its waters flowing back into the Indian Ocean as the Agulhas Return Current (Feron et al., 1992) and feeding the SWIOSG, which forms part of the greater STIOG (Gordon et al., 1987; Stramma and Lutjeharms, 1997) (Fig. 1). Only a relative small proportion of the Agulhas Current's warm and salty waters, approximately 2–15 Sv, are transported into the South Atlantic through the Indian–Atlantic Ocean Gateway via the Agulhas leakage (de Ruijter et al., 1999; Richardson, 2007).

Paleoceanographic studies show that increased input of relatively warm, saline Agulhas Current waters in the South Atlantic are associated with late Pleistocene deglaciations (e.g. Peeters et al., 2004; Martínez-Méndez et al., 2010; Caley et al., 2012; Scussolini and Peeters, 2013). This implies that the transfer of water masses may effectively regulate the buoyancy of the (South) Atlantic Ocean thermocline, and consequently impact the strength of the Atlantic Meridional Overturning Circulation (AMOC) (Weijer et al., 2002; Knorr and Lohmann, 2003). Modelling studies suggest that Agulhas leakage can alter overturning in the North Atlantic on different timescales. The perturbation of planetary waves by Agulhas rings can affect the Atlantic Ocean thermocline on decadal

* Corresponding author. Tel.: +44 (0) 29208 76688.
E-mail address: simonmh@cardiff.ac.uk (M.H. Simon).

0012-821X/$ – see front matter
http://dx.doi.org/10.1016/j.epsl.2013.09.035

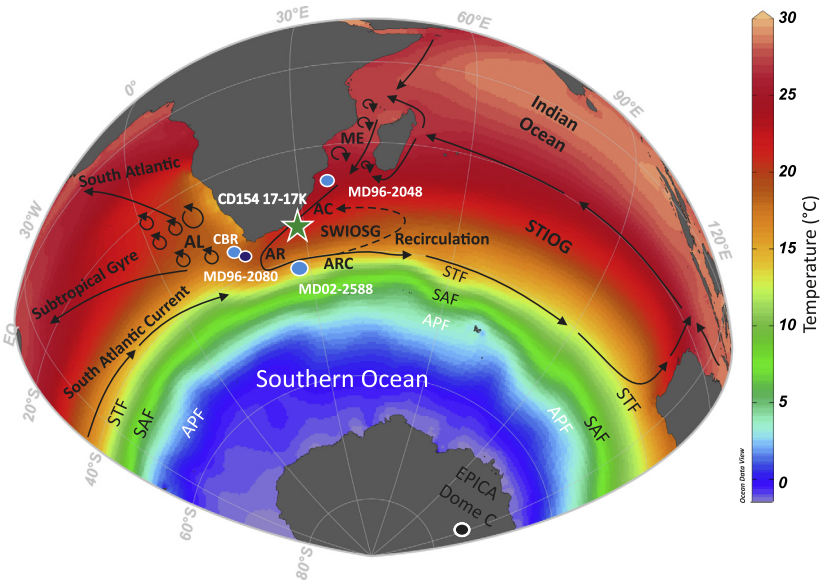

Fig. 1. Location of the Agulhas Current system and palaeoclimate archives used as a reference. Base map illustrates Southern Hemisphere annual mean surface temperatures compiled using the Ocean Data View program (Schlitzer, 2012) and World Ocean Atlas Data 09 (Locarnini et al., 2010). Location of this study is indicated by the star, reference locations are indicated as circles: Agulhas Current (CD154 17-17K, green star, this study), Cape Basin record (CBR, light blue circle, GeoB3603, MD96-2081, Peeters et al., 2004), Agulhas Bank (MD96-2080, dark blue circle, Marino et al., 2013), Agulhas Plateau (MD02-2588, blue circle, Ziegler et al., 2013a), 'precursor' region Agulhas Current (MD96-2048, light blue circle, Caley et al., 2011), Antarctic Ice core (EPICA Dome C, black circle). Black arrows indicate the main surface ocean circulation patterns with emphasis on the key components of the inter-ocean transport across the Agulhas Current system, Agulhas Current (AC), AL (Agulhas leakage in the Agulhas leakage corridor), AR (Agulhas retroflection), ARC (Agulhas Return Current), ME (Mozambique Eddies), STF (Subtropical Front), SAF (Subantarctic front), APF (Antarctic Polar Front), STIOG (Subtropical Indian Ocean gyre), SWIOSG (Southwest Indian Ocean sub-gyre).

timescales, and promote adjustments in the AMOC (Biastoch et al., 2008b; Rühs et al., 2013). While over a period of several hundred years, changes in the buoyancy of the Atlantic thermocline waters, hence salt excess, can influence North Atlantic Deep Water (NADW) formation rates (Weijer et al., 2002; Haarsma et al., 2011). The latter suggests, for example, that a 'saltier' Atlantic ocean due to a more efficient leakage of warm saline Agulhas Current waters, leads to a more stable and potentially stronger AMOC (Weijer et al., 2001, 2002), with implications for global climate.

Most paleo-proxy reconstructions to date have focused on: (1) the Agulhas leakage area in the South Atlantic (Peeters et al., 2004; Martínez-Méndez et al., 2010; Caley et al., 2012; Kasper et al., 2013; Marino et al., 2013); (2) the Agulhas rings pathway in the South Atlantic subtropical gyre (Rackebrandt et al., 2011; Scussolini and Peeters, 2013); (3) outside of the Agulhas Current trajectory (Bard and Rickaby, 2009); or (4) the "precursor" region of the Agulhas Current (Caley et al., 2011) and/or concentrate generally on orbital timescales. Furthermore, studies from the Agulhas leakage corridor that show variability in temperature, salinity and Agulhas leakage fauna (ALF) over time have mainly been interpreted in terms of qualitative changes in the leakage (Peeters et al., 2004; Martínez-Méndez et al., 2010; Caley et al., 2012; Marino et al., 2013). However, importantly it should be recognised that changes in the water mass properties in the Agulhas leakage corridor can be potentially altered either by changes in the amount of water (volume transport) which is transferred through the Indian–Atlantic Ocean Gateway or by hydrographic changes in the upstream Agulhas Current that are subsequently transferred downstream to the Agulhas leakage corridor without altering the actual amount of leakage itself. To date, paleoceanographic oriented studies from the Agulhas leakage corridor have not considered changes in the upstream Agulhas Current to account for the variability seen in the leakage records. To fill this gap, we produced the first high-resolution multi-proxy record from within the main flow of the Agulhas Current (sediment core CD154 17-17K) in the southwest Indian Ocean (Fig. 1).

We examine reconstructions of sea surface temperature (SST), the local oxygen isotope composition of seawater (ice volume corrected $\delta^{18}O_{ivc\text{-}sw}$), which provides an indication of salinity, and foraminiferal assemblage variations from within the main flow of the Agulhas Current. These proxies, when considered in combination, allow hydrographic changes within the current itself to be compared with previously published records from the Agulhas leakage corridor. Our records highlight the importance of considering upstream Agulhas Current variability when explaining Agulhas leakage variability over time.

Model simulations have also tested the sensitivity of the Agulhas Current system to different climatological forcings, such as shifted or intensified Southern Hemisphere westerlies, as well as the impact of the Agulhas Current strength itself on Agulhas leakage (Biastoch et al., 2009a; Rojas et al., 2009; van Sebille et al., 2009; Durgadoo et al., 2013). Additionally, satellite altimetry observations have been used by Backeberg et al. (2012) to suggest that intensified Indian Ocean winds caused enhanced mesoscale variability of the Agulhas Current system, potentially resulting in an increase in Agulhas leakage. These studies emphasise the importance of changes in the Indian Ocean winds fields on Agulhas Current variability and its associated leakage.

Currently, evidence for changes in the strength and position of Southern Hemisphere westerlies during the last glacial cycle, based on both terrestrial and marine paleo-evidence remains equivocal. Reconstructions from the southwest Pacific argue for a maximum in the Southern Hemisphere westerlies during the Last Glacial Maximum (LGM; Shulmeister et al., 2004) and studies from southern South America hint towards a northward movement of the westerly storm tracks during the LGM (Lamy et al., 1998, 1999). In a recent synthesis by Kohfeld et al. (2013), however, it was concluded that the position and strength of Southern Hemisphere westerlies during the LGM remains inconclusive based on data reconstructions alone. Model simulations also remain unclear regarding the position and strength of the Southern Hemisphere westerlies during the LGM. General circulation model (GCM) simulations by Wyrwoll et al. (2000) found evidence for a poleward displace-

ment of the westerlies under glacial conditions, while Rojas et al. (2009) conclude that the Southern Hemisphere westerlies were weaker and less zonally symmetric during the LGM. Recently, Sime et al. (2013) suggest that an equatorward shift of the Southern Hemisphere westerlies of more than three degrees during the LGM was unlikely based on their atmospheric modelling study.

Nevertheless, increased emphasis has been placed on the impact of the Southern Hemisphere westerlies on Agulhas leakage and its consequences for AMOC stability (e.g. Beal et al., 2011 and references therein). Reduced Agulhas leakage during the LGM compared to today has been inferred from a decrease in the proportion of ALF recorded in the CBR (Peeters et al., 2004) and linked to equatorward shifts in the position of the subtropical front (STF) and the Southern Hemisphere westerlies (Bard and Rickaby, 2009). However, reductions in Agulhas leakage may also be associated with strengthened Southern Hemisphere westerlies (Beal et al., 2011; Nof et al., 2011). This underscores the fact that our present understanding of the impacts on the Agulhas Current system of changes in the strength and position of the Southern Hemisphere westerlies is incomplete. We have therefore performed a suite of experiments using an 'ocean only' model of the Agulhas Current system subjected to an equatorward shift and strengthening of the Southern Hemisphere westerlies, both scenarios representative of plausible LGM conditions. This approach provides an idealised framework under which potential paleo-scenarios may be interpreted and allows, at least, a first order approximation for comparison with our proxy reconstructions.

2. Materials and methods

2.1. Core location and oceanography

Marine sediment core CD154 17-17K (33°19.2′S; 29°28.2′E; 3333 m water depth) was recovered from the Natal Valley, south west Indian Ocean during the *RRS Charles Darwin* Cruise 154 (Hall and Zahn, 2004). The core site is located on a contourite sediment drift that has been plastered to the lower continental slope under the influence of NADW. The Natal Valley forms part of the main entry route for NADW exiting the Atlantic at depth before entering the Mozambique and the Somali Basins, then flowing on into the Indian Ocean (van Aken et al., 2004).

Surface waters at the site are within the main trajectory of the upstream 'northern' Agulhas Current where it follows a near rectilinear path along the narrow shelf and steep continental slope (Lutjeharms, 2006). The waters forming the Agulhas Current are sourced from the Red and Arabian Seas, the Indonesian Throughflow, the equatorial Indian Ocean via Mozambique Channel eddies and the East Madagascar Current, and the recirculation of the Agulhas Current (Beal et al., 2006) (Fig. 1). The upper 1000 m of flow within the Mozambique Channel and the southern limb of the East Madagascar Current contribute only ∼5 and 20 Sv respectively to the overall Agulhas Current transport (Donohue and Toole, 2003; Ridderinkhof and de Ruijter, 2003), whereas about 35 Sv is derived from the recirculation of waters within the SWIOSG (Gordon et al., 1987; Stramma and Lutjeharms, 1997), (Fig. 1). These water masses comprise recirculated Indian Ocean waters, which peel off the Agulhas Return Current west of 70°E (Lutjeharms, 2006), and Antarctic Intermediate Waters (AAIW) injected northward into the STIOG at about 60°E (Fine, 1993). These return waters not only contribute most to the volume transport of the Agulhas Current, but they also provide an important control on the surface water properties and dynamics of the current itself (Gründlingh, 1978; Gordon et al., 1987; Stramma and Lutjeharms, 1997; Lutjeharms and Ansorge, 2001; Boebel et al., 2003; Lutjeharms, 2006; Hermes et al., 2007).

2.2. Age model CD 154 17-17K

We use the age model for sediment core CD154 17-17K presented by Ziegler et al. (2013b). In summary, the age model is based on a combination of eight mono-specific planktonic foraminiferal (*Globigerinoides ruber*) radiocarbon dates within the upper part of the record (<40 kyr) and additional graphical correlation of the *G. ruber* stable oxygen isotope (δ^{18}O) record to the Deuterium (temperature) record of Antarctic ice core EPICA Dome C (EPICA, 2004) on the Speleo-age model of Barker et al. (2011). In order to provide a detailed millennial-scale resolution age model, Ziegler et al. (2013b) further fine-tuned the CD154 17-17K age model by visually matching common transitions within the Fe/K ratio of the core and the δ^{18}O speleothem records from Chinese Caves, Hulu (Wang et al., 2001) and Sanbao (Wang et al., 2008). The average age difference between the two independent age models (low resolution planktonic δ^{18}O-based tuning and high resolution Fe/K-based tuning) is minor and demonstrates that the Fe/K tuning approach provides a robust millennial-scale resolution stratigraphic framework. According to this age model sediment core CD154 17-17K spans approximately the last 100 kyr (MIS 1-5c), with an average linear sedimentation rate of 4 cm/kyr, ranging between 2 to 5 cm/kyr.

2.3. Planktonic foraminifera δ^{18}O and Mg/Ca measurements

We use combined stable oxygen isotope (δ^{18}O) and Mg/Ca measurements in the planktonic foraminifera species *G. ruber* (sensu stricto) to reconstruct changes in the surface hydrography of the Agulhas Current (Fig. 2). Around 30–60 individuals were picked from the 250–315 μm size fraction every 2 cm along core CD154 17-17K (3.6 m total length) providing a temporal resolution of ∼0.5 kyr over the last 100 kyr.

G. ruber is a typical warm water species, which is highly abundant in the tropical–subtropical waters of the Indian Ocean and makes up to 40–60% of the planktonic foraminiferal assemblage of the Agulhas Current today. *G. ruber* is a spinose, symbiont-bearing species which inhabits surface (0–50 m) waters (Fairbanks et al., 1980; Erez and Honjo, 1981; Hemleben et al., 1986; Ravelo and Fairbanks, 1992; Peeters and Brummer, 2002; Peeters et al., 2002). A study of calcification depths of planktonic foraminifera in the tropical Indian Ocean showed that *G. ruber* calcifies within the mixed-layer, between 20–50 m (Mohtadi et al., 2009).

Stable isotopes were measured using either a ThermoFinnigan MAT 252 mass spectrometer linked online to a Carbo Kiel-II carbonate preparation device or a Thermo Scientific Delta V Advantage mass spectrometer coupled with a Gas Bench III automated preparation device depending on the sample size. Measurements of δ^{18}O were determined relative to the Vienna Peedee Belemnite scale (VPDB) through calibration with the NBS-19 carbonate standard, with a long-term external precision for both instruments better than ±0.08‰.

Samples for Mg/Ca analysis were prepared and cleaned following the protocol outlined by Barker et al. (2003). The samples were analysed using a Thermo Element XR High Resolution Inductive Coupled Plasma Mass Spectrometry with a long-term precision of element ratios, determined by replicate analyses of standard solutions containing Mg/Ca = 1.15 mmol mol^{-1} and Mg/Ca = 6.9 mmol mol^{-1}, of ±1.25% and ±0.52% respectively. Additional information regarding quality control for the Mg/Ca measurements is provided in the supplementary information (SF. 1a, b).

The Mg/Ca ratios of *G. ruber* were converted to calcification temperature (SST) using the calibration by Anand et al. (2003): $[T = (1/0.09) * \ln(\mathrm{Mg/Ca}/0.449)]$. The standard error associated with this calibration is ±1.1 °C on the SST estimates. We use the Anand et al. (2003) Mg/Ca thermometry equation because (i) the

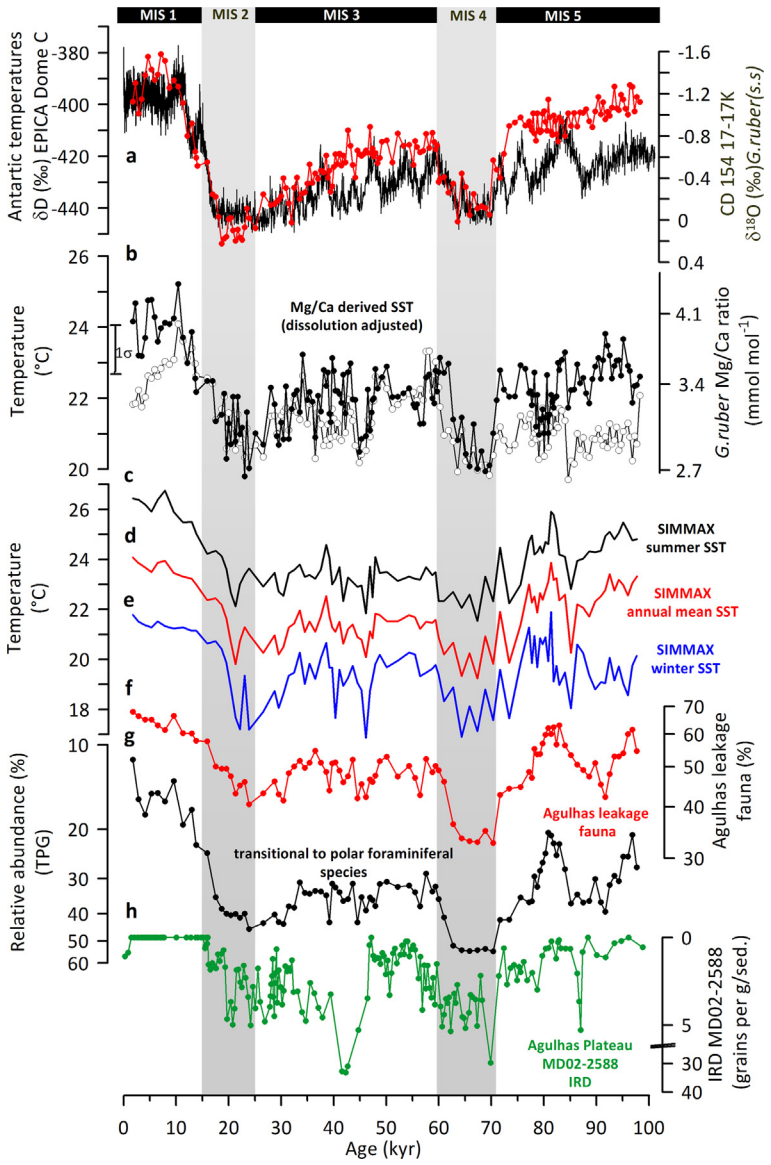

Fig. 2. Comparison of past hydrographic changes in the upstream Agulhas Current (CD154 17-17K) with hydrographic changes in the Southern Ocean and temperatures over Antarctica. Data is shown in comparison with other regional and global climate records. (a) Antarctic temperatures δD (black), (EPICA DOME C) and planktonic foraminiferal (*G. ruber*) δ^{18}O record from CD15417-17K, (red) (b) *G. ruber* Mg/Ca ratios and derived SSTs (white) and dissolution adjusted SSTs, (black) (c) SIMMAX method derived summer/warm season SSTs, (black) (d) SIMMAX method derived annual mean SSTs, (red) (e) SIMMAX method derived winter/cold season SSTs, (blue) (f) tropical–subtropical planktonic foraminifera marker species (Agulhas leakage fauna, ALF), (logarithmic scale, red) (g) relative abundance of transitional to polar foraminifera species group (TPG), *G. inflata*, *N. pachyderma* (dex+sin), *G. bulloides* and *G. truncatulinoides* (dex+sin) as an indicator of southern sourced/transitional water mass influence on the core site and strength of recirculation, (inverted logarithmic scale, black) (h) IRD record of core MD02-2588 from Agulhas Plateau, (green). Error bar represents the 1σ propagated error for the Mg/Ca-derived temperature reconstructions.

calibration used foraminifera tests from a very similar size fraction as our study and (ii) inter-laboratory comparisons have shown that Mg/Ca results are dependent on the procedure used to clean foraminifera shells (Rosenthal et al., 2004) and, similar to this study, Anand et al. (2003) used the cleaning procedure from Barker et al. (2003).

Mg/Ca content of foraminiferal calcite is particularly sensitive to dissolution (Rosenthal et al., 2004; Barker et al., 2005). We therefore apply the dissolution adjustment of Rosenthal and Lohmann (2002) in which the pre-exponential constant of the paleothermometry equation is adjusted as a function of the shell weight of *G. ruber*: $Mg/Ca_{G.ruber} = (0.025\ wt + 0.11)\ e^{0.095T}$ (see supplementary information for details). Full error propagation (combined error of analytical, cleaning procedure, calibration and natural variability uncertainty) yields 1σ uncertainty for our Mg/Ca derived SST estimates of $\pm$1.21 °C.

2.4. Seawater oxygen isotope reconstruction ($\delta^{18}O_{sw}$)

The Mg/Ca derived *G. ruber* calcification temperatures were used to determine the oxygen isotopic composition of seawater ($\delta^{18}O_{sw}$) by extracting the temperature component from the δ^{18}O of the calcite using the paleotemperature equation of Kim and O'Neil (1997), with a VPDB to Standard Mean Ocean Water (SMOW) δ^{18}O correction of 0.27‰ (Hut, 1987). Applying this approach in this study using late Holocene (0–5 kyr) values yields a $\delta^{18}O_{sw}$ of 0.62‰ ($\pm$0.3‰, propagated error) which is consistent with the 0.60‰ ($\pm$0.1‰, 1σ standard deviation) derived from modern seawater observations in the subtropical Indian Ocean between 24°S to 43°S (Tiwari et al., 2013).

We corrected the $\delta^{18}O_{sw}$ for changes in global ice-volume to produce ice-volume corrected local $\delta^{18}O_{sw}$ estimates ($\delta^{18}O_{ivc\text{-}sw}$) following Grant et al. (2012) assuming a glacial δ^{18}O-enrichment

in seawater of 0.008‰ per meter sea level lowering (Schrag et al., 2002). The global $\delta^{18}O_{sw}$ records were synchronized with our planktonic $\delta^{18}O$ record by optimizing their graphical fit. This was done to minimize stratigraphic misfits between the global $\delta^{18}O_{sw}$ and our local record that would potentially generate artefacts in the computed local $\delta^{18}O_{ivc\text{-}sw}$ record. Full error propagation yields 1σ uncertainties for our $\delta^{18}O_{ivc\text{-}sw}$ data of ± 0.3‰.

2.5. Planktonic foraminiferal census counts, Agulhas leakage fauna

The species composition of planktonic foraminiferal assemblages are sensitive to upper water column conditions including SST (Morey et al., 2005) and are used to provide additional constraints on the Agulhas Current variability. The size fraction >150 μm was split to yield a minimum of 350 individuals, and the abundance of the most dominant species relative to the total planktonic foraminiferal assemblage were calculated every 4 cm.

We generated SST estimates from the assemblages using the modern analog technique with similarity index (SIMMAX) transfer function following the approach described in Pflaumann et al. (1996) (Fig. 2c–e, SF. 1c–d). The SIMMAX technique uses a modern calibration dataset to correlate foraminiferal assemblages with known SST estimates, then compares downcore assemblages with the calibration dataset using a similarity equation from Pflaumann et al. (1996). Here we have employed an additional step by performing a logarithmic transformation of the downcore and calibration datasets, which yields an improvement in the resulting SST estimation. Using this approach the standard deviation of residuals is 0.99 °C for the global database, and the estimation of the annual mean temperature is 1.0 °C and 0.9 °C for the South Atlantic Ocean and Indian Ocean, respectively (SF. 1c–d). The original percentage and log-transformed databases were tested by calculating the SST for both the global database and for individual ocean sectors (e.g. South Atlantic Ocean; Indian Ocean), using each sector as a discrete dataset. Here, SST estimates were calculated by assessing the similarity of modern day core top assemblages with the down core assemblages of CD154 17-17K, thereby choosing the mean of the ten closest modern analogues. We used the MARGO dataset (Kucera et al., 2005; Waelbroeck et al., 2009) as the reference database, and used present day annual mean and seasonal SST values from the World Ocean Atlas 1998 (NOAA) measurements. The dataset includes further core top samples to increase coverage of modern day analogues in the Agulhas region. Annual average, summer/warm season and winter/cold season sea surface temperatures were estimated. The annual average SST estimates resemble the Mg/Ca derived SST data of *G. ruber* in terms of both temperature range and variability (Fig. 2b, d).

The Agulhas leakage fauna proxy (ALF) is considered to reflect the intensity of past Indian–Atlantic water exchange via Agulhas leakage in the South Atlantic (Peeters et al., 2004). The quantification of the ALF assemblage in the upstream Agulhas Current is important in evaluating the connection between the upstream variability and the downstream response within the Agulhas leakage corridor. To calculate the ALF index in CD154 17-17K, the sum of the relative abundance of the species *Pulleniatina obliquiloculata, Globigerinita glutinata, Hastigerina pelagica, Globorotalia menardii, Globigerinoides sacculifer, Globigerinella siphonifera, Globigerinoides ruber, Orbulina universa, Globoquadrina hexagona* and *Globorotalia scitula* was taken.

Species which are presently found at higher latitudes, i.e. associated with colder water masses near the dynamic STF (Graham et al., 2012), or further south in polar waters, have been defined here as the transitional to polar group (TPG) which includes the species *Neogloboquadrina pachyderma* (dex+sin), *Globorotalia inflata, Globigerinoides bulloides and Globorotalia truncatulinodes* (dex+sin) (Peeters et al., 2004).

2.6. Ice-rafted debris

In order to identify northward shifts of the Southern Ocean frontal system we use iceberg rafted debris (IRD) occurrence recorded at the southern Agulhas Plateau located eight degrees further to the south of our core location (Fig. 1). Lithic fragments (>150 μm fraction) were counted in marine sediment core MD02-2588, (41°19.9′S; 25°49.4′E; 2907 m water depth) every 2 cm between Marine Isotope Stages (MIS) 1–5. The results are expressed as grains per gram of dry sediment (grains/g sed) (Fig. 2h). The data are shown on their independent age model for core MD02-2588 (Ziegler et al., 2013a).

2.7. Numerical model simulations

We analysed a sub-domain of a regional eddy-permitting model of the greater Agulhas Current system, AGIO. This configuration has been demonstrated to realistically simulate the complicated circulation around South Africa (Loveday et al., submitted for publication) (Fig. 4). AGIO is a 1/4°, eddy-permitting representation of the Indian Ocean basin, produced using v. 2.1 of the Regional Ocean Modelling System (ROMS) (Shchepetkin and McWilliams, 2005) and constructed with ROMSTOOLS (Penven et al., 2008). The model simulates the large-scale features of the Indian Ocean and regional transport in the Agulhas source regions. Using the methodology described in Bryden et al. (2005), AGIO records an Agulhas Current volume transport of 76.9 ± 19.9 Sv, consistent with the 78.6 ± 19.9 Sv observed over the same section (Bryden et al., 2005; Biastoch et al., 2009b). Here, as the CD154 17-17K Agulhas core lies at 33°S, Agulhas transport estimates are calculated from the barotropic stream function along a transect that spans the core site on a line perpendicular from the shore to the first recirculation (AC33, Fig. 4a).

The low numerical viscosity of ROMS allows for a well-captured eddy field at this resolution. Eddy kinetic energy (EKE) patterns in the source regions and at the retroflection are well represented. Low viscosity also reduces viscous choking at the retroflection, allowing inertia to govern the local dynamic (Dijkstra and de Ruijter, 2001). AGIO estimates an Agulhas leakage of 27.6 ± 2.8 Sv through quantifying the Eulerian flux of an Indian Ocean passive tracer across the Cape Basin.

AGIO was bulk forced by the CORE v. 2b normal year surface fluxes (Large and Yeager, 2009). Modification of the wind field in the sensitivity experiments was achieved through the addition of anomalies that modify the zonal component of the westerly wind stress (see Loveday et al., submitted for publication and Durgadoo et al., 2013, for full methodology), (Fig. 4b). Anomalies were based on the reference zonal wind-stress between 20°E and 115°E, but were applied across the model domain. Two sensitivity experiments were performed, one in which the westerly wind-stress was increased by 40% (Wp40), and the other where the westerly winds were shifted equatorward by 4 degrees (Nth4).

Reference boundary conditions were supplied by a 1/2° ORCA05 reference run (Biastoch et al., 2008a), also forced with CORE v. 2b normal year fluxes. Boundary conditions for the Wp40 and Nth4 sensitivity experiment were derived from ORCA05 runs forced with the appropriate wind stress changes applied throughout the Southern Hemisphere (Durgadoo et al., 2013).

3. Results

The $\delta^{18}O_{G.ruber}$ profile of the Agulhas Current core CD154 17-17K displays clear orbital modulations, with glacial–interglacial amplitudes of 1‰ to 1.8‰ during MIS 5a/4 transition and Termination I (TI), respectively (Fig. 2a). Superimposed on the orbital oscillations is higher frequency variability that alludes to millennial-

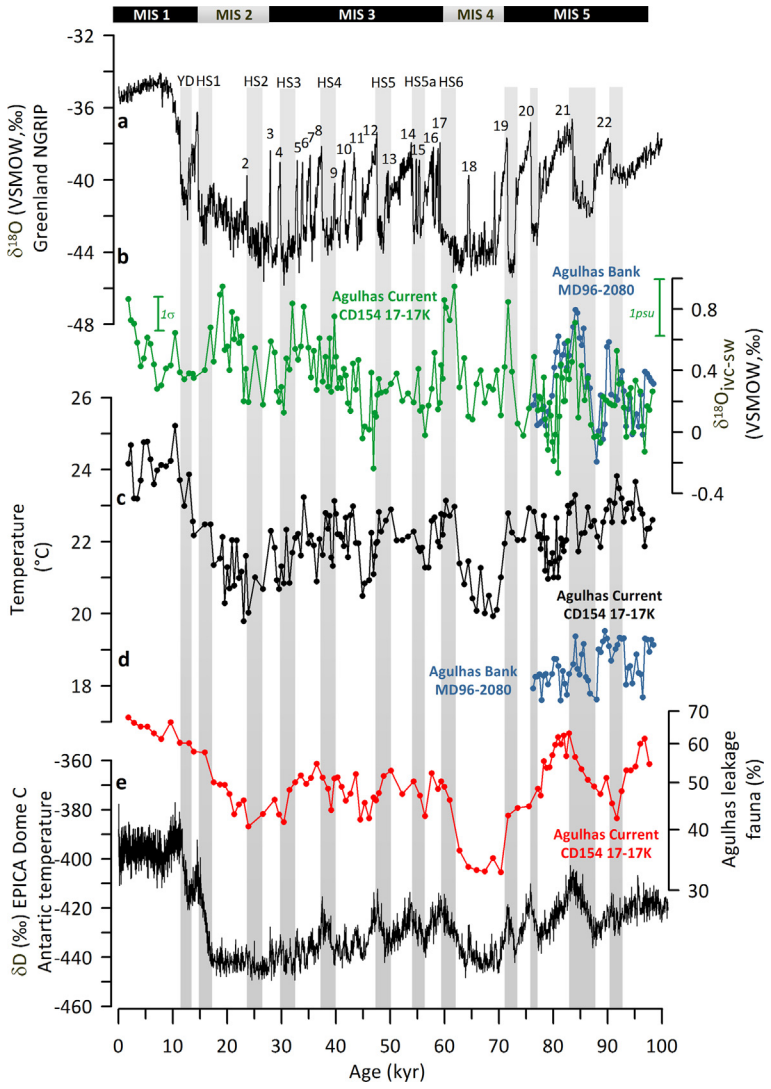

Fig. 3. Comparison of millennial-scale climate change in Greenland with surface water changes in the SW Indian Ocean since 100 kyr. (a) δ^{18}O record from Greenland ice core NGRIP, (black), (NGRIP, 2004) displaying abrupt temperature variability in the North Atlantic (cold Northern Hemisphere intervals and Heinrich Stadials are marked as grey bars), numbers indicate warm D/O interstadials (b) ice-volume corrected $\delta^{18}O_{SW}$ reconstruction ($\delta^{18}O_{ivc-sw}$) based on *G. ruber* Mg/Ca-derived SSTs, (green); $\delta^{18}O_{ivc-sw}$ reconstructions of Agulhas Bank record (MD96-2080, blue, Marino et al., 2013) is shown in comparison (c) dissolution adjusted SSTs based on *G. ruber* Mg/Ca ratios, (black); SSTs of Agulhas Bank record (MD96-2080, blue, Marino et al., 2013) is shown in comparison (d) relative abundance of tropical–subtropical planktonic foraminifera marker species, (logarithmic scale, red), (Agulhas leakage fauna, ALF) (e) Antarctic temperatures δD, (black), (EPICA Dome C, (EPICA, 2004)). Error bar represents the 1σ propagated error for the $\delta^{18}O_{ivc-sw}$ reconstructions and estimated equivalent changes translated into salinity units following Tiwari et al. (2013).

scale shifts in the surface water hydrography of the Agulhas Current, even if somewhat less pronounced.

The SST variations inferred from the $Mg/Ca_{G.ruber}$ record (Fig. 2b) and SIMMAX method derived annual, summer/warm season and winter/cold season temperatures (Fig. 2c–e) also show a distinct glacial–interglacial pattern. An obvious feature within the record is the cooling into MIS 4 and 2 when winter SSTs decrease to 17 °C and Mg/Ca based SST reconstructions suggest SSTs of 20 °C. Warm conditions (23–26 °C) during the interglacial MIS 5 and the Holocene co-vary with highest percentages of tropical–subtropical foraminiferal species (ALF) varying between 40–65% (Fig. 2b–f).

Throughout the entire record intervals of high abundances of TPG species from transitional/frontal water masses (Fig. 2g) co-vary with pronounced cooling events and high IRD accumulation rates at the Agulhas Plateau (Fig. 2h). The IRD deposition rates in core MD02-2588 are quite variable over the past 100 kyr and generally resemble the temperature pattern of the Agulhas Current, with less IRD deposited at the Agulhas Plateau during times of warmer SSTs recorded at CD154 17-17K and vice versa (Fig. 2b–e, h). Notably, within MIS 4 (~70 kyr), the SST cooling of up to 4 °C coincides with peak IRD deposition rates of 30 grains/g sed (Fig. 2b, h).

The SST and $\delta^{18}O_{ivc-sw}$ profiles from the Agulhas Current display clear millennial-scale variability with abrupt increases up to 2 °C and ~0.8‰ (~2 psu) respectively, aligning with Northern Hemisphere cold events (NGRIP, 2004) (Fig. 3a–c). Synchronously, ALF abundances rise by about 15% at the same time mostly resembling features recorded in the Antarctic temperature record (Fig. 3d, e). Notably, the Northern Hemisphere stadial cooling that precedes 'Dansgaard–Oeschger' (D-O) events 21 and 19 (Dansgaard et al., 1993), as well as Heinrich Stadial (HS) 6 (Heinrich, 1988) are key examples of intervals of more warm, saline conditions on millennial timescales (Fig. 3a, b, c).

Data associated with this article can be found in the supplementary information.

3.1. Modelling results

In order to better understand the mechanism driving the large orbital to millennial-scale surface waters changes in the Agulhas

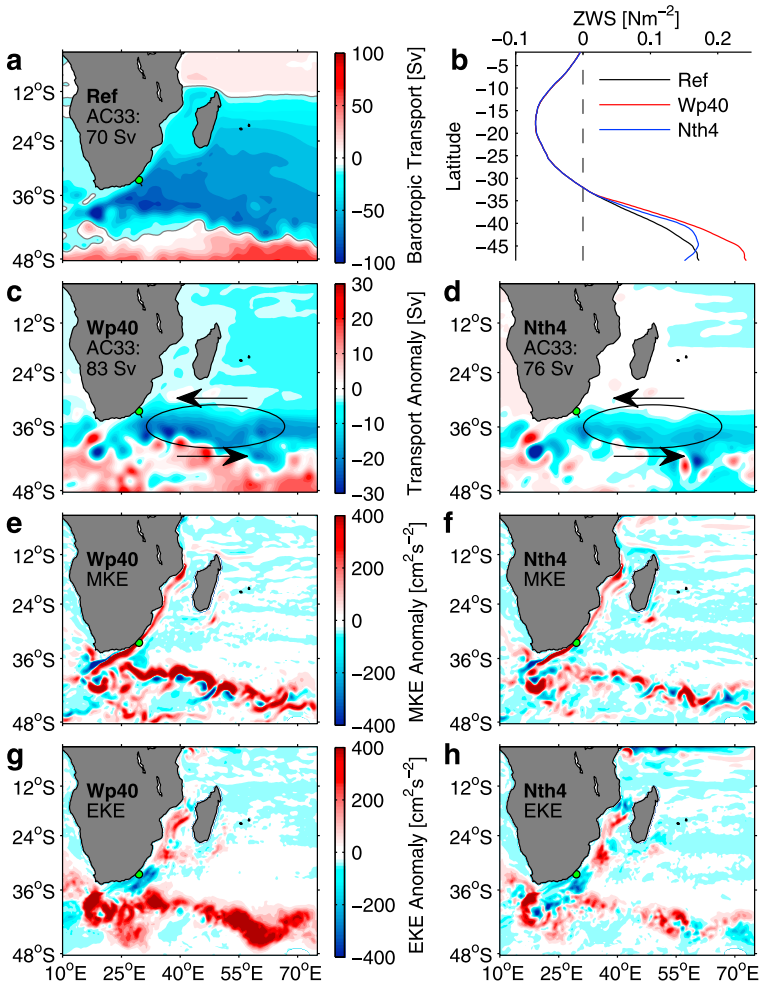

Fig. 4. Changes in regional transport and mesoscale variability with Indian Ocean wind-stress. (a) The barotropic transport function for the southwest Indian Ocean, as extracted from the AGIO climatological reference experiment. The green dot shows the core site. The barotropic AC33 transport is measured across the Agulhas Current along a transect perpendicular to the shore, bisecting the core site. The grey line nominally separates cyclonic (red) from anti-cyclonic (blue) flow. (b) The mean zonal wind-stress across the Indian Ocean between 20°E and 115°E, for the regional Wp40 and Nth4 sensitivity experiments. (c, d) The anomaly in the barotropic transport (sensitivity – reference) associated with the Wp40 and Nth4 experiments, respectively. The black ellipse highlights the increase in anti-cyclonic circulation in the STIOG and SWIOSG (e, g) the respective anomalies in the 20-yr mean (MKE) and eddy kinetic energy (EKE) fields for the Wp40 case. (f, h) as in (e, g), but for the Nth4 experiment.

Current observed in our proxy reconstructions we utilise the results of our idealised model experiments.

The sensitivity of regional Agulhas transport to basin-scale intensification or an equatorward shift of the westerly wind changes is clearly highlighted in Fig. 4c–d, which shows the respective anomalies in the barotropic transport function as compared to the reference state (Fig. 4a). Anti-cyclonic flow in the sub-gyre, shown in blue shading and highlighted with the black ellipse, is more intense when winds are strengthened (Fig. 4c), although both sensitivity experiments show increases in the local recirculation (Fig. 4d) with increased wind-stress at 40°S (Fig. 4b). This enhancement in wind stress (and wind stress curl) at 40°S drives an increase in northward transport, forcing an intensification of the SWIOSG, and an enhancement of local circulation.

The SWIOSG intensification augments the recirculation component of the Agulhas Current, but only significantly impacts the flow south of 32°S. At 33°S, the CD154 17-17K Agulhas core location, barotropic transport anomalies for the Wp40 and Nth4 cases are 13 Sv and 6 Sv, respectively (Fig. 4c, d). The contributions from the northern source regions (e.g. Mozambique Channel and East Madagascar Current) remain largely unchanged. Panels e to h of Fig. 4 shows the anomalies in mean (MKE) and eddy (EKE) kinetic energy for the two sensitivity experiments. In both cases, the Agulhas Current south of 33°S, Agulhas retroflection and Agulhas Return Current shows large increases in MKE (Fig. 4e, f), consistent with higher transports. In the northern Agulhas Current, around the core site, there is a decrease in EKE, suggesting that the current becomes less variable here (Fig. 4g, h). However, the EKE increases at the retroflection, and in the Agulhas Return Current. The response to the changes in wind-shift are much more pronounced in the case of the Wp40 experiment (Fig. 4h), due to the larger change in wind stress applied in this experiment (Fig. 4b).

4. Discussion

4.1. Long-term and millennial-scale variability of the Agulhas Current – linking changes in the Agulhas Current with Agulhas leakage variability

Our high-resolution multi-proxy record from the Agulhas Current provides insights into the nature and timing of the hydrography and climatic variability of the wider Agulhas Current system, with distinct variability on both orbital as well as millennial timescales over the past 100 kyr. In order to compare this variability with the reconstructions of the Agulhas leakage from the Agulhas corridor, Cape Basin Record (CBR; Peeters et al., 2004), we have used the benthic δ^{18}O records to synchronise the CBR to the CD154 17-17K age scale (Fig. 5a). Major SST decreases which are accompanied by decreasing abundances in the ALF can be recog-

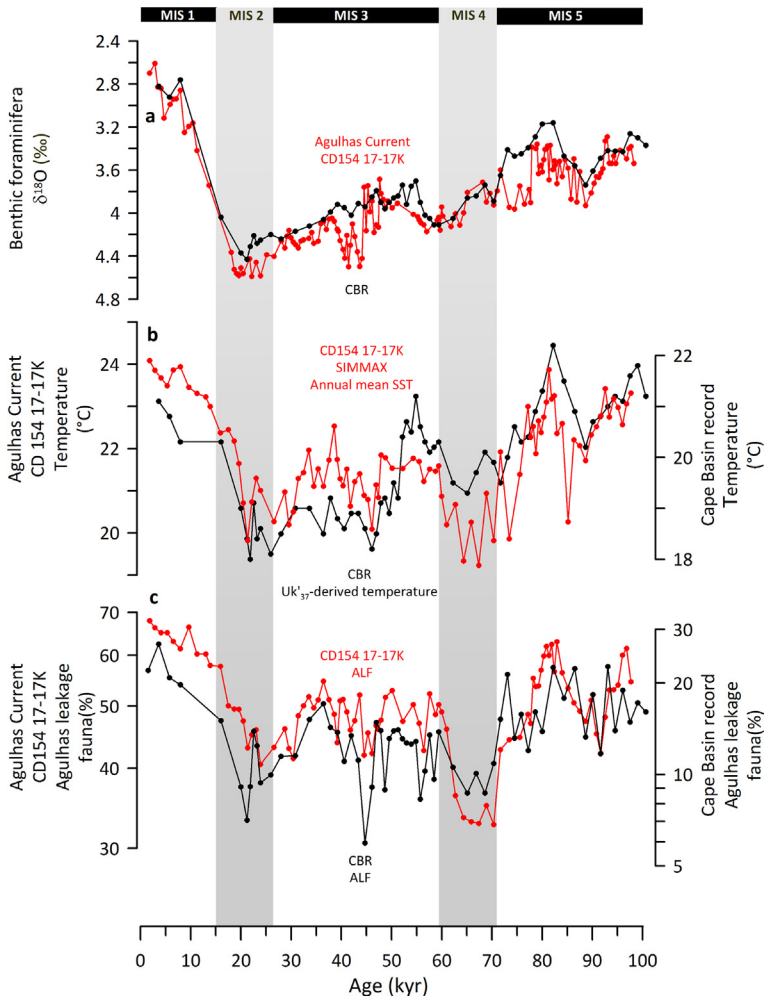

Fig. 5. Comparison between the upstream Agulhas Current (CD154 17-17K) variability over the past 100 kyr and Agulhas leakage. (a) benthic foraminifera $\delta^{18}O$ records in comparison to age model alignment (CD154 17-17K, red, CBR, black) (b) annual mean SIMMAX method derived SSTs in the Agulhas Current (CD154 17-17K, red) and Uk'_{37} derived SSTs in the Agulhas leakage corridor (CBR, black, Peeters et al., 2004) (c) relative abundance of tropical–subtropical planktonic foraminiferal marker species (Agulhas leakage fauna, ALF) in the upstream Agulhas Current (CD154 17-17K, logarithmic scale, red) and in the Agulhas leakage corridor (CBR, logarithmic scale, black).

nised in both regions throughout the entire record (Fig. 5b, c). Notably, during the last deglaciation, both regions show an SST increase of ~3°C with ALF abundance increasing from ~40–65% and 7–27% at the CD154 17-17K and CBR sites respectively (Fig. 5b, c). The similarities between these records strongly implies that changing environmental conditions impacted the wider Agulhas Current simultaneously and suggests a close connection between upstream Agulhas Current variability and its transmission further downstream within the Agulhas leakage corridor.

To date a lack of proxy records from the Agulhas leakage corridor and the Agulhas Current resolving millennial-scale resolution has prevented a direct comparison between these two areas. However, a recently published high-resolution record from the Agulhas Bank, South Atlantic (Marino et al., 2013) (sediment core MD96-2080, 36°19.2′S, 19°28.2′E, 2488 m water depth, Fig. 1) spanning MIS 5–8 offers the opportunity to compare both locations on millennial-scale basis, as both records overlap during the period between 76–98 kyr. Importantly, Marino et al. (2013) also use the same planktonic foraminiferal species (*G. ruber*) to monitor changes in temperature and $\delta^{18}O_{ivc\text{-}sw}$ as our study, therefore avoiding the complications arising from comparing signals of differing foraminiferal species. The MD96-2080 record displays two distinct $\delta^{18}O_{ivc\text{-}sw}$ maxima during this time interval at 87–84 kyr and at 94–90 kyr, defined in their study as Agulhas Salt-leakage Maxima (ASM), ASM 21 and 22 with $\delta^{18}O_{sw}$ increases of ~1‰ and 0.6‰, respectively. Both $\delta^{18}O_{ivc\text{-}sw}$ anomalies are accompanied by temperature increases of up to ~2 °C. Similar oscillations, within the combined age uncertainties, are recorded in the upstream Agulhas Current during these intervals with positive $\delta^{18}O_{ivc\text{-}sw}$ excursions of 0.7‰ at 87–84 kyr and 0.5‰ at 94–90 kyr (Fig. 3b) and temperature increases of up to 1.5 °C (Fig. 3c). However, even considering analytical uncertainties, the $\delta^{18}O_{ivc\text{-}sw}$ and SSTs excursions in the Agulhas Bank record appear slightly more pronounced compared to our core site in the SW Indian Ocean. The reason for these differences is unclear but could be related to changes in the oceanographic setting of the core sites, which may affect the sensitivity of the geochemical proxies. Nevertheless, the striking correspondence of the observed variability in SST, ALF abundances and $\delta^{18}O_{ivc\text{-}sw}$ in both areas suggests that the documented surface water signals recorded in the Agulhas leakage area are representative of changes in the wider Agulhas Current system as a whole, or plausibly form in the upstream Agulhas Current and are transmitted to the downstream region by the current itself.

Millennial-scale SST, ALF and $\delta^{18}O_{ivc\text{-}sw}$ changes in the Agulhas Current align with Northern Hemisphere cold events (i.e., Heinrich events; Fig. 3). The increases in these features during maximum cooling in the North Atlantic, peak in step with the rapid shifts to interstadial conditions in Greenland (Fig. 3a), and abruptly decreases shortly thereafter. Examples of this phasing in the Agulhas Current, among others, are seen at 87–84 kyr, and at

63–59 kyr, where the temperature, ALF and salinity build-up in the Agulhas Current parallels the cold stadial conditions in the north (Fig. 3a–d). These intervals suggest an interhemispheric teleconnection between millennial-scale climate variability in the North Atlantic and observed changes in the Agulhas Current. These findings are consistent with the 'bipolar seesaw' pattern of Northern Hemisphere cooling and Southern Hemisphere warming during the last glacial period (Broecker, 1998; Stocker and Johnsen, 2003; Barker et al., 2009). Such a pattern has been explained by changes in the cross-equatorial heat flux connected to variability of the AMOC (Knutti et al., 2004).

Millennial-scale warming events, revealing an out-of-phase relationship with stadial conditions in the North Atlantic, have also been observed elsewhere within the Indian Ocean and suggest that the oscillations of the Agulhas Current are likely coherent with the wider regional bipolar response. Mg/Ca-derived SST records from the Indonesian Throughflow region immediately south of Indonesia (Levi et al., 2007) indicate a temperature increase of about 2 °C during HS2, HS1 and the Younger Dryas (YD). Faunal assemblage based SST estimates from a core site in the Mozambique Channel (Levi et al., 2007) display warming during HS1 and YD of about 1.5 °C. The Indonesian Throughflow and the Mozambique Channel are considered important source water areas supplying the Agulhas Current (Beal et al., 2011). A more recent study by De Deckker et al. (2012) show millennial-scale warm phases south of Australia during HS1-3 and YD with temperature increases between 1.5–3 °C during these intervals. Millennial-scale warm phases south of Australia are linked in their study to the position of the dynamic STF which is determined by latitudinal shifts of the Southern Hemisphere westerlies. A study from the Antarctica zone in the Pacific Ocean (Anderson et al., 2009), based on opal deposition events, further infers latitudinal shifts of the Southern Hemisphere westerlies during millennial-scale, Northern Hemisphere cold events.

Numerical modelling simulations suggest that in response to a North Atlantic cold event the Hadley Cell in the southern tropics weakens which ultimately strengthens and/or shifts the Southern Hemisphere westerlies towards Antarctica (Toggweiler and Lea, 2010; Lee et al., 2011). However, a recent study by Sime et al. (2013) challenges the link between the strength of the Hadley Cell and the associated impact on the westerlies. Nevertheless, these findings suggest that the reorganisation of the atmospheric circulation, position and strength of the Southern Hemisphere westerlies, during Northern Hemisphere cold events might have played an important role in determining the bipolar warming response of the Southern Ocean. We therefore further explore the response and sensitivity of the Agulhas Current system to shifted Southern Hemisphere westerlies.

4.2. Southwest Indian Ocean sub-gyre dynamics and its impact on Agulhas Return Current variability

Coldest upper ocean conditions in the Agulhas Current prevailed during MIS 4 and 2/3 boundary (Fig. 2). These intervals are marked by a reduced abundance of the ALF and a higher proportion of TPG associated with polar to transitional water masses. Ice-rafted debris events at the Agulhas Plateau have been interpreted as indicating episodes of intensified northward advection of polar waters associated with the northward shift of regional oceanic fronts supporting iceberg survivability as far north as the Agulhas Plateau, 41°S (Fig. 1). Increased IRD is closely related to the local cooling events observed in the upstream Agulhas Current (Fig. 2b, h) implying a tight coupling between both regions. We suggest that the synchronous cooling events of both areas are related to changes in the dynamics of SWIOSG and associated Agulhas Return Current that allowed a stronger influence of colder southern component surface waters to modify the hydrography of the upstream Agulhas Current. Cold, transitional water masses occurring along the dynamic STF are entrained into the Agulhas Return Current due to the recurrent eddy generation and shifts in its trajectory that closely follows the front (Lutjeharms and Ansorge, 2001) (Fig. 1).

Evidence from our numerical model simulations strongly suggests a strengthening and zonal expansion of the SWIOSG under intensified or equatorward-shifted Southern Hemisphere westerlies (Fig. 4c, d). Additionally, the increase in wind stress curl south of 35°S in both cases results in an enhancement of the transport in the Agulhas Return Current. This stronger transport is reflected in both the MKE and EKE immediately north of the STF (Fig. 4e–h). Increasing EKE reflects an enhanced prevalence or propagation speed of mesoscale features, such as eddies and meanders. The increase in turbulence associated with these features may facilitate increased cross frontal mixing by weakening the thermal gradients associated with the STF, resulting in increased export of Indian Ocean waters to the south, and entrainment of Southern Ocean derived water masses into the Agulhas Return Current. Such a scenario could enable a redistribution of these waters into the Agulhas Current itself via enhanced recirculation leading to the SST cooling and increase in abundance of the TPG observed in the CD154 17-17K record. Equally, theses cold(er) Southern Ocean derived waters would also influence the surface waters near the Agulhas Plateau, potentially enabling increased iceberg survivability in the region. Conversely, warm periods during which sea surface salinities are increased and warm tropical Indian Ocean foraminifera dominate the waters of the Agulhas Current, the influence of the Agulhas Return Current recirculation on the CD154 17-17K site is likely to have been reduced. A suggested southward displacement (or weakening) of the Southern Hemisphere westerlies during Northern Hemisphere cold events and interglacials, which is in agreement with previous studies (Lamy et al., 2004, 2007), would create a less vigorous SWIOSG diminishing the influence of cold, transitional water masses on the Agulhas Current. The lowest IRD accumulation rates at the Agulhas Plateau, indicative of a southward contraction of the Subantarctic zone and associated frontal system, strengthen the assumption that both areas were less affected by southern sourced waters at these times.

A comparison of our record with data by Caley et al. (2011), from the 'precursor' region of the Agulhas Current (sediment core MD96-2048, 26°S, 660 m water depth, Fig. 1), provides further evidence of the Agulhas Current sensitivity to changes in the intensity and influence of the SWIOSG. The lower temporal resolution of the Caley et al. (2011) record, which spans the past 800 kyr, only allows comparison at orbital (glacial–interglacial) timescales, following the synchronisation of the $\delta^{18}O_{G.ruber}$ record of MD96-2048 to the CD154 17-17K age scale (SF. 3a). The $\delta^{18}O_{G.ruber}$ records (SF. 3a) from both sites exhibit prominent glacial–interglacial modulation, for example during the warm conditions of MIS 5a, 3 and the Holocene, where the $\delta^{18}O_{G.ruber}$ records show similar absolute isotopic values. The decoupling of $\delta^{18}O$ values of both records during the cold periods of MIS4 and 2 indicate generally cooler conditions in the Agulhas Current, highlighted by heavier $\delta^{18}O$ values in the CD154 17-17K core, and further supported by the comparison of the Mg/Ca (*G. ruber*) derived SSTs of both records (SF. 3a, b). The varying temperature contrasts between these two areas are most likely a result of changes in the intensity and impact of the SWIOSG on the Agulhas Current. Such that during periods when the SWIOSG was more vigorous, the Agulhas Current at 33°S experienced a stronger influence of cold, transitional waters masses while the 'precursor' regions located further to the north, upstream of the main Agulhas system, remained outside the direct influence of the Agulhas Return Current. Such a scenario would augment the temperature difference between both core locations. Conversely, a less intense SWIOSG would explain the observed similarities and

reduced temperature contrast between both sites observed during warm interglacial conditions. Our results demonstrate that the surface water properties of the Agulhas Current are particularly sensitive to SWIOSG-variability, and the signature of this variability is subsequently transferred into the South Atlantic via Agulhas leakage.

The interplay between waters feeding the Agulhas, either originating from the Southern Ocean frontal system or the tropical Indian Ocean, demonstrates the potential sensitivity of the Agulhas Current hydrography towards varying source influences. This also highlights the different response patterns of the Agulhas Current, one being connected with Southern Hemisphere warming in response to the bipolar seesaw during North Atlantic cold episodes, and the other being connected with a shifted ocean circulation pattern in the SWIOSG in response to a modified atmospheric circulation.

5. Conclusions

Upper ocean temperature, salinity and planktonic foraminiferal assemblage records from the Agulhas Current exhibit a high variability on orbital to millennial timescales. Agulhas leakage records (Peeters et al., 2004; Marino et al., 2013), show a high degree of similarity in this variability and phasing of temperature, salinity and planktonic foraminiferal-based Agulhas leakage. The observed orbital and millennial-scale SST, ALF and salinity oscillations of the Agulhas Current can largely be explained by the bipolar seesaw response of the Indian Ocean itself and the varying influence of the SWIOSG on the Agulhas Current system. A present lack of records of equivalent temporal resolution and stratigraphic reach from within the source areas of the Agulhas Current as well as in the wider STIOG prevent a clear separation between the two dominant forcing mechanisms (westerlies vs. low-latitude tropical Indian Ocean/Pacific) which ultimately determine Agulhas Current variability and its interfered leakage.

Our findings suggest that the temperature and salinity changes in the Agulhas leakage corridor is at least partly a result of upstream variability in these properties within the source region of the Agulhas leakage. The observed changes in the Agulhas leakage corridor might not be necessarily related to changes in the amount of water being transferred through the Indian–Atlantic Ocean Gateway via the Agulhas leakage but rather a consequence of changes in the composition of the Agulhas Current itself. This highlights the care that must be taken when interpreting Agulhas salt-leakage from the Agulhas corridor alone.

Additionally, similarities of our SST record of the past 100 kyr in the Agulhas Current, SW Indian Ocean and the Agulhas Plateau suggest a strong connection between the two regions on both orbital and millennial timescales. As the most plausible mechanism we suggest a transfer of Southern Ocean temperature anomalies via the Agulhas Return Current.

Our modelling exercise demonstrates that increased Agulhas Return Current dynamics and recirculation can be explained by changes in the strength of the SWIOSG forced by either a northward displacement or strengthening of the Southern Hemisphere westerlies. Coldest upper ocean temperatures occurred during MIS4 and MIS2/3 boundary in the Agulhas Current and are accompanied by an increased abundance of Southern Ocean TPG foraminiferal species. During these periods the SWIOSG was likely intensified, causing an enhanced Agulhas Return Current transport and recirculation south of Madagascar. This enhanced Agulhas Return Current allows cold, transitional water masses originating from the frontal zones further to the south to become entrained, and upon reaching the Agulhas Current potentially influence its hydrographic properties. This implies that the large-scale wind fields (Southern Hemisphere westerlies) over the subtropical Indian Ocean are one of the main controls on the Agulhas Current variability with consequences for Atlantic surface waters buoyancy as well as AMOC stability.

Acknowledgements

We acknowledge funding from the European Commission 7th Framework Marie Curie People programme FP7/2007-2013 through funding of the Initial Training Network 'GATEWAYS' (www.gatewaysitn.eu) under the grant number 238512 and the Climate Change Consortium of Wales. We thank the Captain, officers and crew of *RRS Charles Darwin* Cruise number 154, for which IH and RZ also gratefully acknowledge funding support from the Natural Environment Research Council. Furthermore we acknowledge funding from the DAAD (German Academic Exchange Service) which supported the RISE (Research Internships in Science and Engineering) internship placement of Teresa Neff who assisted in carrying out laboratory and analytical work on core material CD154 17-17K. G. Rothwell and S. Maclachlan facilitated access and the measurement of CD154-17-17K on the ITRAX XRF scanning system at BOSCORF, National Oceanographic Centre, Southampton, UK. We thank all those colleagues who generously made published data available, either directly or through NOAA data centre for Palaeoclimatology and PANGAEA. Julia Becker and Anabel Morte-Ródenas provided technical support with the isotope and trace element analysis at Cardiff University. We thank J. Durgadoo for providing the ORCA05 OGCM boundary conditions for our regional wind shift experiments. We thank Jamie Wilson, Emily Deaney and Paola Moffa Sanchez for useful discussions and acknowledge the two anonymous reviewers for their constructive comments, which helped us to improve the manuscript.

Appendix A. Supplementary material

Supplementary material related to this article can be found online at http://dx.doi.org/10.1016/j.epsl.2013.09.035.

References

Anand, P., Elderfield, H., Conte, M.H., 2003. Calibration of Mg/Ca thermometry in planktonic foraminifera from a sediment trap time series. Paleoceanography 18, 1050.

Anderson, R.F., Ali, S., Bradtmiller, L.I., Nielsen, S.H.H., Fleisher, M.Q., Anderson, B.E., Burckle, L.H., 2009. Wind-driven upwelling in the Southern Ocean and the deglacial rise in atmospheric CO_2. Science 323, 1443–1448.

Backeberg, B.C., Penven, P., Rouault, M., 2012. Impact of intensified Indian Ocean winds on mesoscale variability in the Agulhas system. Nat. Clim. Change 2, 608–612.

Bard, E.a., Rickaby, R.E.M., 2009. Migration of the subtropical front as a modulator of glacial climate. Nature 460, 380–383.

Barker, S., Greaves, M., Elderfield, H., 2003. A study of cleaning procedures used for foraminiferal Mg/Ca paleothermometry. Geochem. Geophys. Geosyst. 4, 8407.

Barker, S., Cacho, I., Benway, H., Tachikawa, K., 2005. Planktonic foraminiferal Mg/Ca as a proxy for past oceanic temperatures: a methodological overview and data compilation for the Last Glacial Maximum. Quat. Sci. Rev. 24, 821–834.

Barker, S., Diz, P., Vautravers, M.J., Pike, J., Knorr, G., Hall, I.R., Broecker, W.S., 2009. Interhemispheric Atlantic seesaw response during the last deglaciation. Nature 457, 1097–1102.

Barker, S., Knorr, G., Edwards, R.L., Parrenin, F., Putnam, A.E., Skinner, L.C., Wolff, E., Ziegler, M., 2011. 800,000 years of abrupt climate variability. Science 334, 347–351.

Beal, L.M., Chereskin, T.K., Lenn, Y.D., Elipot, S., 2006. The sources and mixing characteristics of the Agulhas Current. J. Phys. Oceanogr. 36, 2060–2074.

Beal, L.M., De Ruijter, W.P.M., Biastoch, A., Zahn, R., 2011. On the role of the Agulhas system in ocean circulation and climate. Nature 472, 429–436.

Biastoch, A., Böning, C.W., Getzlaff, J., Molines, J.-M., Madec, G., 2008a. Causes of interannual–decadal variability in the meridional overturning circulation of the midlatitude North Atlantic Ocean. J. Climate 21, 6599–6615.

Biastoch, A., Boning, C.W., Lutjeharms, J.R.E., 2008b. Agulhas leakage dynamics affects decadal variability in Atlantic overturning circulation. Nature 456, 489–492.

Biastoch, A., Boning, C.W., Schwarzkopf, F.U., Lutjeharms, J.R.E., 2009a. Increase in Agulhas leakage due to poleward shift of Southern Hemisphere westerlies. Nature 462, 495–498.
Biastoch, A., Beal, L., Lutjeharms, J., Casal, T., 2009b. Variability and coherence of the Agulhas Undercurrent in a high-resolution ocean general circulation model. J. Phys. Oceanogr. 39 (10), 2417–2435.
Boebel, O., Rossby, T., Lutjeharms, J., Zenk, W., Barron, C., 2003. Path and variability of the Agulhas Return Current. Deep-Sea Res., Part 2, Top. Stud. Oceanogr. 50, 35–56.
Broecker, W.S., 1998. Paleocean circulation during the Last Deglaciation: A bipolar seesaw?. Paleoceanography 13, 119–121.
Bryden, H., Beal, L., Duncan, L., 2005. Structure and transport of the Agulhas Current and its temporal variability. J. Oceanogr. 61, 479–492.
Caley, T., Kim, J.H., Malaizé, B., Giraudeau, J., Laepple, T., Caillon, N., Charlier, K., Rebaubier, H., Rossignol, L., Castañeda, I.S., Schouten, S., Damsté, J.S.S., 2011. High-latitude obliquity forcing as a dominant forcing in the Agulhas current system. Clim. Past 7, 1285–1296.
Caley, T., Giraudeau, J., Malaizé, B., Rossignol, L., Pierre, C., 2012. Agulhas leakage as a key process in the modes of Quaternary climate changes. Proc. Natl. Acad. Sci. 109, 6835–6839.
Dansgaard, W., Johnsen, S.J., Clausen, H.B., Dahl-Jensen, D., Gundestrup, N.S., Hammer, C.U., Hvidberg, C.S., Steffensen, J.P., Sveinbjornsdottir, A.E., Jouzel, J., Bond, G., 1993. Evidence for general instability of past climate from a 250-kyr ice-core record. Nature 364, 218–220.
De Deckker, P., Moros, M., Perner, K., Jansen, E., 2012. Influence of the tropics and southern westerlies on glacial interhemispheric asymmetry. Nat. Geosci. 5, 266–269.
de Ruijter, W.P.M., Biastoch, A., Drijfhout, S.S., Lutjeharms, J.R.E., Matano, R.P., Pichevin, T., Leeuwen, P.J.v., Weijer, W., 1999. Indian–Atlantic interocean exchange: Dynamics, estimation and impact. J. Geophys. Res. 104, 20,885–20,910.
Dijkstra, H.A., de Ruijter, W.P.M., 2001. On the physics of the Agulhas Current: steady retroflection regimes. J. Phys. Oceanogr. 31, 2971–2985.
Donohue, K.A., Toole, J.M., 2003. A near-synoptic survey of the Southwest Indian Ocean. Deep-Sea Res., Part 2, Top. Stud. Oceanogr. 50, 1893–1931.
Durgadoo, J.V., Loveday, B.R., Reason, C.J.C., Penven, P., Biastoch, A., 2013. Agulhas Leakage predominantly responds to the Southern Hemisphere westerlies. J. Phys. Oceanogr, http://dx.doi.org/10.1175/JPO-D-13-047.1.
EPICA, 2004. Eight glacial cycles from an Antarctic ice core. Nature 429, 623–628.
Erez, J., Honjo, S., 1981. Comparison of isotopic composition of planktonic foraminifera in plankton tows, sediment traps and sediments. Palaeogeogr. Palaeoclimatol. Palaeoecol. 33, 129–156.
Fairbanks, R.G., Wiebe, P.H., BÉ, A.W.H., 1980. Vertical distribution and isotopic composition of living planktonic foraminifera in the Western North Atlantic. Science 207, 61–63.
Feron, R.C.V., De Ruijter, W.P.M., Oskam, D., 1992. Ring shedding in the Agulhas Current System. J. Geophys. Res. 97, 9467–9477.
Fine, R.A., 1993. Circulation of Antarctic intermediate water in the South Indian Ocean. Deep-Sea Res., Part 1, Oceanogr. Res. Pap. 40, 2021–2042.
Gordon, A.L., Lutjeharms, J.R.E., Gründlingh, M.L., 1987. Stratification and circulation at the Agulhas Retroflection. Deep-Sea Res., Part 1, Oceanogr. Res. Pap. 34, 565–599.
Graham, R.M., de Boer, A.M., Heywood, K.J., Chapman, M.R., Stevens, D.P., 2012. Southern Ocean fronts: Controlled by wind or topography?. J. Geophys. Res. 117, C08018.
Grant, K.M., Rohling, E.J., Bar-Matthews, M., Ayalon, A., Medina-Elizalde, M., Ramsey, C.B., Satow, C., Roberts, A.P., 2012. Rapid coupling between ice volume and polar temperature over the past 150,000 years. Nature 491, 744–747.
Gründlingh, M.L., 1978. Drift of a satellite-tracked buoy in the southern Agulhas Current and Agulhas Return Current. Deep-Sea Res. 25, 1209–1224.
Haarsma, R., Campos, E.D., Drijfhout, S., Hazeleger, W., Severijns, C., 2011. Impacts of interruption of the Agulhas leakage on the tropical Atlantic in coupled ocean–atmosphere simulations. Clim. Dyn. 36, 989–1003.
Hall, I.R., Zahn, R., 2004. Cruise Report RRS Charles Darwin Cruise 154: 13/12/2003–10/01/2004, Durban to Cape Town, South Africa, Agulhas 'Leakage' and Abrupt Climate Change.
Heinrich, H., 1988. Origin and consequences of cyclic ice rafting in the Northeast Atlantic Ocean during the past 130,000 years. Quat. Res. 29, 142–152.
Hemleben, C., Spindler, M., Anderson, O.R. (Eds.), 1986. Modern Planktonic Foraminifera. Springer-Verlag, New York. 363 pp.
Hermes, J.C., Reason, C.J.C., Lutjeharms, J.R.E., 2007. Modeling the variability of the greater Agulhas Current system. J. Climate 20, 3131–3146.
Hut, G., 1987. Consultants' group meeting on stable isotope reference samples for geochemical and hydrological investigations. In: Rep. to Dir. Gen.. Vienna, 16–18 September 1985. Int. At. Energy Agency, Vienna, p. 42.
Kasper, S., van der Meer, M.T.J., Mets, A., Zahn, R., Sinninghe Damsté, J.S., Schouten, S., 2013. Salinity changes in the Agulhas leakage area recorded by stable hydrogen isotopes of C37 alkenones during Termination I and II. Clim. Past Discuss. 9, 3209–3238.
Kim, S.-T., O'Neil, J.R., 1997. Equilibrium and nonequilibrium oxygen isotope effects in synthetic carbonates. Geochim. Cosmochim. Acta 61, 3461–3475.
Knorr, G., Lohmann, G., 2003. Southern Ocean origin for the resumption of Atlantic thermohaline circulation during deglaciation. Nature 424, 532–536.
Knutti, R., Fluckiger, J., Stocker, T.F., Timmermann, A., 2004. Strong hemispheric coupling of glacial climate through freshwater discharge and ocean circulation. Nature 430, 851–856.
Kohfeld, K.E., Graham, R.M., Boer, A.M.d., Sime, L.C., Wolff, E.W., Quéré, C.L., Bopp, L., 2013. Southern Hemisphere westerly wind changes during the Last Glacial Maximum: Paleo-data synthesis. Quat. Sci. Rev. 64, 104–120, http://dx.doi.org/10.1016/j.quascirev.2012.12.008.
Kucera, M., Weinelt, M., Kiefer, T., Pflaumann, U., Hayes, A., Weinelt, M., Chen, M.-T., Mix, A.C., Barrows, T.T., Cortijo, E., Duprat, J., Juggins, S., Waelbroeck, C., 2005. Reconstruction of sea-surface temperatures from assemblages of planktonic foraminifera: multi-technique approach based on geographically constrained calibration data sets and its application to glacial Atlantic and Pacific Oceans. Quat. Sci. Rev. 24, 951–998.
Lamy, F., Hebbeln, D., Wefer, G., 1998. Late Quaternary precessional cycles of terrigenous sediment input off the Norte Chico, Chile (27.5°S) and palaeoclimatic implications. Palaeogeogr. Palaeoclimatol. Palaeoecol. 141, 233–251.
Lamy, F., Hebbeln, D., Wefer, G., 1999. High-resolution marine record of climatic change in mid-latitude Chile during the last 28,000 years based on Terrigenous sediment parameters. Quat. Res. 51, 83–93.
Lamy, F., Kaiser, J., Ninnemann, U., Hebbeln, D., Arz, H.W., Stoner, J., 2004. Antarctic timing of surface water changes off Chile and Patagonian ice sheet response. Science 304, 1959–1962.
Lamy, F., Kaiser, J., Arz, H.W., Hebbeln, D., Ninnemann, U., Timm, O., Timmermann, A., Toggweiler, J.R., 2007. Modulation of the bipolar seesaw in the Southeast Pacific during Termination 1. Earth Planet. Sci. Lett. 259, 400–413.
Large, W.G., Yeager, S.G., 2009. The global climatology of an interannually varying air–sea flux data set. Clim. Dyn. 33, 341–364.
Lee, S.-Y., Chiang, J.C.H., Matsumoto, K., Tokos, K.S., 2011. Southern Ocean wind response to North Atlantic cooling and the rise in atmospheric CO_2: Modeling perspective and paleoceanographic implications. Paleoceanography 26, PA1214.
Levi, C., Labeyrie, L., Bassinot, F., Guichard, F., Cortijo, E., Waelbroeck, C., Caillon, N., Duprat, J., de Garidel-Thoron, T., Elderfield, H., 2007. Low-latitude hydrological cycle and rapid climate changes during the last deglaciation. Geochem. Geophys. Geosyst. 8, Q05N12.
Locarnini, R.A., Mishonov, A.V., Antonov, J.I., Boyer, T.P., Garcia, H.E., Baranova, O.K., Zweng, M.M., Johnson, a.D.R, 2010. World Ocean Atlas 2009 Volume 1: Temperature. In: Levitus, S. (Ed.), NOAA Atlas NESDIS, vol. 68. U.S. Government Printing Office, Washington, DC, 184 pp.
Loveday, B.R., Durgadoo, J.V., Reason, C.J.C., Biastoch, A.a., Penven, P., submitted for publication. Decoupling of the Agulhas leakage from the Agulhas Current. J. Phys. Oceanogr.
Lutjeharms, J.R.E., 2006. Three decades of research on the greater Agulhas Current. Ocean Sci. Discuss. 3, 939–995.
Lutjeharms, J.R.E., Ansorge, I.J., 2001. The Agulhas Return Current. J. Mar. Syst. 30, 115–138.
Marino, G., Zahn, R., Ziegler, M., Purcell, C., Knorr, G., Hall, I.R., Ziveri, P., Elderfield, H., 2013. Agulhas salt-leakage oscillations during abrupt climate changes of the Late Pleistocene. Paleoceanography, http://dx.doi.org/10.1002/palo.20038.
Martínez-Méndez, G., Zahn, R., Hall, I.R., Peeters, F.J.C., Pena, L.D., Cacho, I., Negre, C., 2010. Contrasting multiproxy reconstructions of surface ocean hydrography in the Agulhas Corridor and implications for the Agulhas Leakage during the last 345,000 years. Paleoceanography 25, PA4227.
Mohtadi, M., Steinke, S., Groeneveld, J., Fink, H.G., Rixen, T., Hebbeln, D., Donner, B., Herunadi, B., 2009. Low-latitude control on seasonal and interannual changes in planktonic foraminiferal flux and shell geochemistry off south Java: A sediment trap study. Paleoceanography 24, PA1201.
Morey, A.E., Mix, A.C., Pisias, N.G., 2005. Planktonic foraminiferal assemblages preserved in surface sediments correspond to multiple environment variables. Quat. Sci. Rev. 24, 925–950.
NGRIP, 2004. High-resolution record of Northern Hemisphere climate extending into the last interglacial period. Nature 431, 147–151.
Nof, D., Zharkov, V., Ortiz, J., Paldor, N., Arruda, W., Chassignet, E., 2011. The arrested Agulhas retroflection. J. Mar. Res. 69, 659–691.
Peeters, F.J.C., Brummer, G.-J.A., 2002. The Seasonal and Vertical Distribution of Living Planktic Foraminifera in the NW Arabian Sea. Special Publications, vol. 195. Geological Society, London, pp. 463–497.
Peeters, F.J.C., Brummer, G.-J.A., Ganssen, G., 2002. The effect of upwelling on the distribution and stable isotope composition of Globigerina bulloides and Globigerinoides ruber (planktic foraminifera) in modern surface waters of the NW Arabian Sea. Glob. Planet. Change 34, 269–291.
Peeters, F.J.C., Acheson, R., Brummer, G.-J.A., de Ruijter, W.P.M., Schneider, R.R., Ganssen, G.M., Ufkes, E., Kroon, D., 2004. Vigorous exchange between the Indian and Atlantic oceans at the end of the past five glacial periods. Nature 430, 661–665.
Penven, P., Marchesiello, P., Debreu, L., Lefèvre, J., 2008. Software tools for pre- and post-processing of oceanic regional simulations. Environ. Model. Softw. 23, 660–662.

Pflaumann, U., Duprat, J., Pujol, C., Labeyrie, L.D., 1996. SIMMAX: A modern analog technique to deduce Atlantic sea surface temperatures from planktonic foraminifera in deep-sea sediments. Paleoceanography 11, 15–35.

Rackebrandt, N., Kuhnert, H., Groeneveld, J., Bickert, T., 2011. Persisting maximum Agulhas leakage during MIS 14 indicated by massive Ethmodiscus oozes in the subtropical South Atlantic. Paleoceanography 26, PA3202.

Ravelo, A.C., Fairbanks, R.G., 1992. Oxygen isotopic composition of multiple species of planktonic foraminifera: recorders of the modern photic zone temperature gradient. Paleoceanography 7, 815–831.

Richardson, P.L., 2007. Agulhas leakage into the Atlantic estimated with subsurface floats and surface drifters. Deep-Sea Res., Part 1, Oceanogr. Res. Pap. 54, 1361–1389.

Ridderinkhof, H., de Ruijter, W.P.M., 2003. Moored current observations in the Mozambique Channel. Deep-Sea Res., Part 2, Top. Stud. Oceanogr. 50, 1933–1955.

Rojas, M., Moreno, P., Kageyama, M., Crucifix, M., Hewitt, C., Abe-Ouchi, A., Ohgaito, R., Brady, E., Hope, P., 2009. The Southern Westerlies during the last glacial maximum in PMIP2 simulations. Clim. Dyn. 32, 525–548.

Rosenthal, Y., Lohmann, G.P., 2002. Accurate estimation of sea surface temperatures using dissolution-corrected calibrations for Mg/Ca paleothermometry. Paleoceanography 17, 1044.

Rosenthal, Y., Perron-Cashman, S., Lear, C.H., Bard, E., Barker, S., Billups, K., Bryan, M., Delaney, M.L., deMenocal, P.B., Dwyer, G.S., Elderfield, H., German, C.R., Greaves, M., Lea, D.W., Marchitto, T.M., Pak, D.K., Paradis, G.L., Russell, A.D., Schneider, R.R., Scheiderich, K., Stott, L., Tachikawa, K., Tappa, E., Thunell, R., Wara, M., Weldeab, S., Wilson, P.A., 2004. Interlaboratory comparison study of Mg/Ca and Sr/Ca measurements in planktonic foraminifera for paleoceanographic research. Geochem. Geophys. Geosyst. 5, Q04D09.

Rühs, S., Durgadoo, J.V., Behrens, E., Biastoch, A., 2013. Advective timescales and pathways of Agulhas leakage. Geophys. Res. Lett. 40, 3997–4000.

Schlitzer, R., 2012. Ocean Data View, http://odv.awi.de.

Schrag, D.P., Adkins, J.F., McIntyre, K., Alexander, J.L., Hodell, D.A., Charles, C.D., McManus, J.F., 2002. The oxygen isotopic composition of seawater during the Last Glacial Maximum. Quat. Sci. Rev. 21, 331–342.

Scussolini, P., Peeters, F.J.C., 2013. A record of the last 460 thousand years of upper ocean stratification from the central Walvis Ridge, South Atlantic. Paleoceanography, http://dx.doi.org/10.1002/palo.20041.

Shchepetkin, A.F., McWilliams, J.C., 2005. The regional oceanic modeling system (ROMS): a split-explicit, free-surface, topography-following-coordinate oceanic model. Ocean Model. 9, 347–404.

Shulmeister, J., Goodwin, I., Renwick, J., Harle, K., Armand, L., McGlone, M.S., Cook, E., Dodson, J., Hesse, P.P., Mayewski, P., Curran, M., 2004. The Southern Hemisphere westerlies in the Australasian sector over the last glacial cycle: a synthesis. Quat. Int. 118–119, 23–53.

Sime, L.C., Kohfeld, K.E., Le Quéré, C., Wolff, E.W., de Boer, A.M., Graham, R.M., Bopp, L., 2013. Southern Hemisphere westerly wind changes during the Last Glacial Maximum: model-data comparison. Quat. Sci. Rev. 64, 104–120.

Stocker, T.F., Johnsen, S.J., 2003. A minimum thermodynamic model for the bipolar seesaw. Paleoceanography 18, 1087.

Stramma, L., Lutjeharms, J.R.E., 1997. The flow field of the subtropical gyre of the South Indian Ocean. J. Geophys. Res. 102, 5513–5530.

Tiwari, M., Nagoji, S.S., Kartik, T., Drishya, G., Parvathy, R.K., Rajan, S., 2013. Oxygen isotope–salinity relationships of discrete oceanic regions from India to Antarctica vis-à-vis surface hydrological processes. J. Mar. Syst. 113–114, 88–93.

Toggweiler, J.R., Lea, D.W., 2010. Temperature differences between the hemispheres and ice age climate variability. Paleoceanography 25, PA2212.

van Aken, H.M., Ridderinkhof, H., de Ruijter, W.P.M., 2004. North Atlantic deep water in the south-western Indian Ocean. Deep-Sea Res., Part 1, Oceanogr. Res. Pap. 51, 755–776.

van Sebille, E., Biastoch, A., van Leeuwen, P.J., de Ruijter, W.P.M., 2009. A weaker Agulhas Current leads to more Agulhas leakage. Geophys. Res. Lett. 36, L03601.

Waelbroeck, Paul, Kucera Rosell-Melé, W., Schneider, Mix, Abelmann, Armand, Bard, Barker, Barrows, Benway, Cacho, Chen, Cortijo, Crosta, de Vernal, Dokken, Duprat, Elderfield, Eynaud, Gersonde, Hayes, Henry, Hillaire-Marcel, Huang, Jansen, Juggins, Kallel, Kiefer, Kienast, Labeyrie, Leclaire, Londeix, Mangin, Matthiessen, Marret, Meland, Morey, Mulitza, Pflaumann, Pisias, Radi, Rochon, Rohling, Sbaffi, Schäfer-Neth, Solignac, Spero, Tachikawa, Turon, 2009. Constraints on the magnitude and patterns of ocean cooling at the Last Glacial Maximum. Nat. Geosci. 2, 127–132.

Wang, Y.J., Cheng, H., Edwards, R.L., An, Z.S., Wu, J.Y., Shen, C.C., Dorale, J.A., 2001. A high-resolution absolute-dated late Pleistocene monsoon record from Hulu cave, China. Science 294, 2345–2348.

Wang, Y., Cheng, H., Edwards, R.L., Kong, X., Shao, X., Chen, S., Wu, J., Jiang, X., Wang, X., An, Z., 2008. Millennial- and orbital-scale changes in the East Asian monsoon over the past 224,000 years. Nature 451, 1090–1093.

Weijer, W., De Ruijter, W.P.M., Dijkstra, H.A., 2001. Stability of the Atlantic overturning circulation: competition between Bering Strait Freshwater Flux and Agulhas Heat and Salt Sources. J. Phys. Oceanogr. 31, 2385–2402.

Weijer, W., De Ruijter, W.P.M., Sterl, A., Drijfhout, S.S., 2002. Response of the Atlantic overturning circulation to South Atlantic sources of buoyancy. Glob. Planet. Change 34, 293–311.

Wyrwoll, K.-H., Dong, B., Valdes, P., 2000. On the position of southern hemisphere westerlies at the Last Glacial Maximum: an outline of AGCM simulation results and evaluation of their implications. Quat. Sci. Rev. 19, 881–898.

Ziegler, M., Diz, P., Hall, I.R., Zahn, R., 2013a. Millennial-scale changes in atmospheric CO_2 levels linked to the Southern Ocean carbon isotope gradient and dust flux. Nat. Geosci. 6, 457–461.

Ziegler, M., Simon, M.H., Hall, I.R., Barker, S., Stringer, C., Zahn, R., 2013b. Development of Middle Stone Age innovation linked to rapid climate change. Nat. Commun. 4, 1905.